

# A High-Throughput Functional Screen Identifies Small Molecule Regulators of Temperature- and Mechano-Sensitive $K_{2P}$ Channels

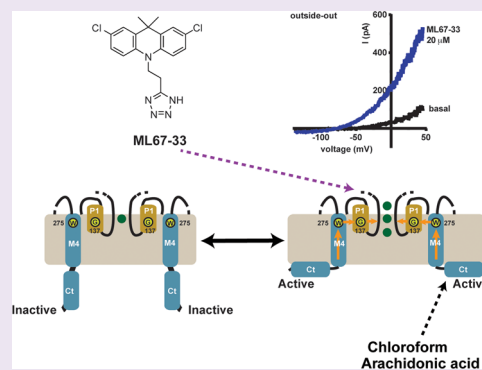
Sviatoslav N. Bagriantsev,<sup>†,‡</sup> Kean-Hooi Ang,<sup>‡</sup> Alejandra Gallardo-Godoy,<sup>‡</sup> Kimberly A. Clark,<sup>†</sup> Michelle R. Arkin,<sup>‡</sup> Adam R. Renslo,<sup>‡</sup> and Daniel L. Minor, Jr.\*<sup>†,‡,§,||,⊥</sup>

<sup>†</sup>Cardiovascular Research Institute, <sup>‡</sup>Small Molecule Discovery Center and Department of Pharmaceutical Chemistry, <sup>§</sup>Departments of Biochemistry and Biophysics and Cellular and Molecular Pharmacology, and <sup>||</sup>California Institute for Quantitative Biomedical Research, University of California, San Francisco, California 94158, United States

<sup>⊥</sup>Physical Biosciences Division, Lawrence Berkeley National Laboratory, Berkeley, California 94720, United States

## S Supporting Information

**ABSTRACT:**  $K_{2P}$  (KCNK) potassium channels generate “leak” potassium currents that strongly influence cellular excitability and contribute to pain, somatosensation, anesthesia, and mood. Despite their physiological importance,  $K_{2P}$ s lack specific pharmacology. Addressing this issue has been complicated by the challenges that the leak nature of  $K_{2P}$  currents poses for electrophysiology-based high-throughput screening strategies. Here, we present a yeast-based high-throughput screening assay that avoids this problem. Using a simple growth-based functional readout, we screened a library of 106,281 small molecules and identified two new inhibitors and three new activators of the mammalian  $K_{2P}$  channel  $K_{2P2.1}$  (*KCNK2*, *TREK-1*). By combining biophysical, structure–activity, and mechanistic analysis, we developed a dihydroacridine analogue, ML67-33, that acts as a low micromolar, selective activator of temperature- and mechano-sensitive  $K_{2P}$  channels. Biophysical studies show that ML67-33 reversibly increases channel currents by activating the extracellular selectivity filter-based C-type gate that forms the core gating apparatus on which a variety of diverse modulatory inputs converge. The new  $K_{2P}$  modulators presented here, together with the yeast-based assay, should enable both mechanistic and physiological studies of  $K_{2P}$  activity and facilitate the discovery and development of other  $K_{2P}$  small molecule modulators.



$K_{2P}$  channels regulate electrical activity in various tissues through generation of a plasma membrane “leak” potassium conductance.<sup>1,2</sup> Channels from this family function in excitable and nonexcitable cells and are implicated in vasodilation, respiratory control, nociception, neuroprotection, anesthesia, and antidepressant responses.<sup>1–3</sup> Due to their involvement in pain, ischemia, and migraine,  $K_{2P}$ s are proposed as targets for a range of cardiovascular and neurological disorders;<sup>3</sup> however, despite this considerable interest, the  $K_{2P}$  family is poorly responsive to classic potassium channel blockers<sup>4</sup> and remains practically pharmacologically orphaned.<sup>2,3</sup> Development of specific  $K_{2P}$  pharmacology has been hindered by the scarcity of facile methods to detect potassium flux in cells and by the fact that the channels produce a voltage-independent “leak” current that is a challenge for conventional electrophysiological screening assays. Thus, there is a need to develop new screening strategies for identifying  $K_{2P}$  modulators.

Here, we report the development and implementation of a high-throughput yeast-based screening assay for small molecule modulators of the polymodal  $K_{2P}$ ,  $K_{2P2.1}$  (*KCNK2*, *TREK-1*).<sup>5–7</sup> This channel is regulated by heat,<sup>8</sup> mechanical force,<sup>9</sup> general anesthetics,<sup>9,10</sup> and G-protein coupled receptors<sup>6</sup> and is involved in pain,<sup>11,12</sup> general anesthetic responses,<sup>13</sup> neuroprotection from ischemia,<sup>13</sup> and depression.<sup>14</sup> Although a

variety of pharmacologic agents affect  $K_{2P2.1}$  (*TREK-1*) function, such as millimolar concentrations of volatile halogenated<sup>4,9,10,15,16</sup> and gaseous general anesthetics,<sup>4,15,17</sup> the neuroprotective agent riluzole (10–100  $\mu$ M),<sup>4,18</sup> and the antidepressant fluoxetine (Prozac) ( $IC_{50}$   $\sim$ 10  $\mu$ M),<sup>4,19,20</sup> these compounds have other molecular targets.<sup>15</sup> Hence, we set out to develop small molecules that could control  $K_{2P2.1}$  (*TREK-1*) activity selectively. Such molecules should serve as tools to dissect the unconventional gating apparatus that controls  $K_{2P2.1}$  (*TREK-1*) function<sup>21–23</sup> and may also provide lead compounds for novel anesthetics, neuroprotectants, and drugs against mood disorders.

Using a yeast-based screen, coupled with electrophysiological analysis, we discovered  $K_{2P2.1}$  (*TREK-1*) inhibitors and activators in a single 106,281 small molecule screening campaign. These modulators comprise different chemical classes and reversibly affect  $K_{2P2.1}$  (*TREK-1*). Beginning with a carbazole-based scaffold present in the activator ML67, we developed ML67-33, an activator that rapidly and reversibly affects  $K_{2P2.1}$  (*TREK-1*) with an  $EC_{50}$  in the low micromolar

Received: April 26, 2013

Accepted: June 6, 2013

Published: June 6, 2013

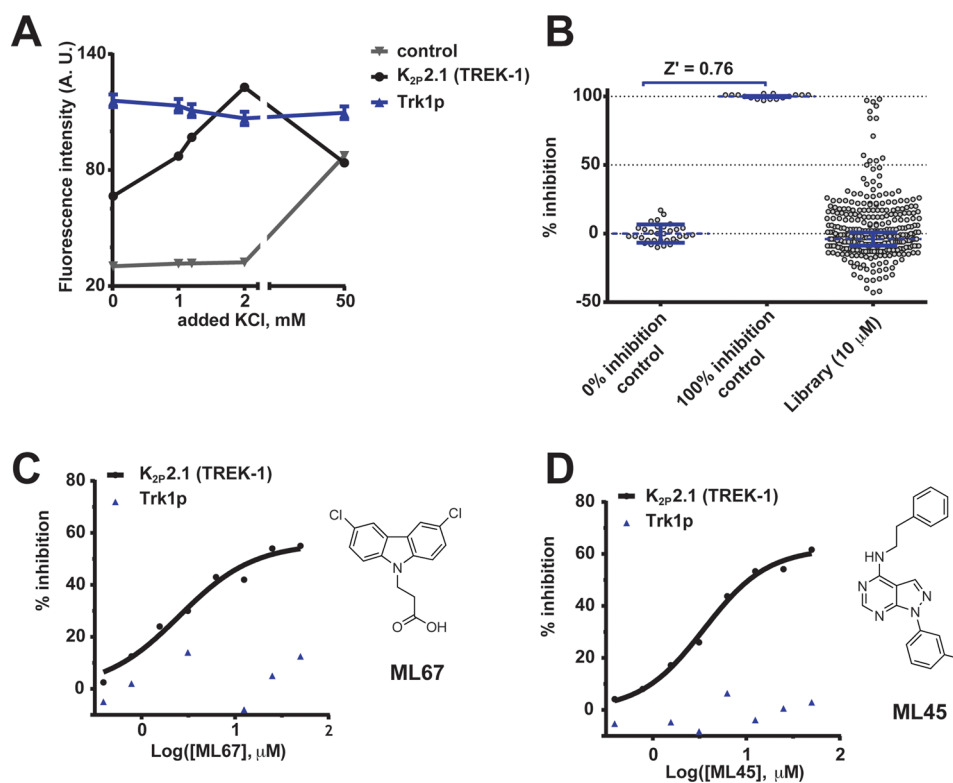


**Figure 1.** Yeast screen identifies K<sub>2p</sub>2.1 (TREK-1) small molecule modulators. (A) Resazurin (Alamar blue) measurement of potassium concentration growth effects on SGY1528 yeast expressing the indicated constructs. Error bars show  $\pm$  SE,  $n = 16$ . For some points, error bars are smaller than symbols. (B) Exemplar scatter plot showing growth inhibition score distribution from a 384-well screening plate. Each point represents end-point normalized resazurin fluorescence. Error bars show  $\pm$  SD. (C, D) Dose–response for (C) ML67 and (D) ML45 on growth inhibition of yeast expressing K<sub>2p</sub>2.1 (TREK-1) (black circles) or Trk1p (blue triangles). Compound structures are shown.

range and by acting on the extracellular C-type gate through a novel mechanism. This dihydroacridine analogue also activates the two temperature- and mechano-sensitive K<sub>2p</sub> channels most closely related to K<sub>2p</sub>2.1 (TREK-1), K<sub>2p</sub>10.1 (TREK-2), and K<sub>2p</sub>4.1 (TRAAK) but has no effects on more distantly related K<sub>2p</sub>s. Thus, ML67-33 represents a novel K<sub>2p</sub> activator that has specificity within the K<sub>2p</sub> family. Our success with this yeast-based assay establishes a new means for discovering K<sub>2p</sub> small molecule modulators.

## RESULTS AND DISCUSSION

**High-Throughput Yeast Screen Identifies K<sub>2p</sub>2.1 (TREK-1) Activators and Inhibitors.** We desired to address the dearth of K<sub>2p</sub> channel pharmacology by developing a high-throughput screen (HTS) for small molecule K<sub>2p</sub> modulators. Prior studies have established that growth of the potassium-uptake-deficient yeast strain SGY1528<sup>24</sup> could be rescued in solid-media assays by ectopic expression of diverse potassium channels,<sup>25–27</sup> including K<sub>2p</sub>2.1 (TREK-1).<sup>22</sup> Although this platform has been used to screen libraries of <10,000 compounds against the inward rectifier Kir2.1<sup>28,29</sup> and has proven advantageous for studying blocker interactions with potassium channels,<sup>27,30</sup> the solid media format limits the scalability for screening large libraries of compounds. Hence, we focused on developing a means to monitor rescue of growth under limiting potassium concentrations by heterologously expressed potassium channels, such as K<sub>2p</sub>2.1 (TREK-1), in a liquid media HTS format.

We measured the signal generated by the vital dye resazurin (Alamar Blue), which live cells convert to a fluorescent form,<sup>31</sup>

to quantify the abundance of living SGY1528 grown in liquid culture in 386-well plates for 24 h in media containing a range of potassium concentrations (Figure 1). When cultured in media containing 0–50 mM KCl, cells expressing the yeast potassium transporter Trk1p<sup>32</sup> exhibited similar levels of resazurin fluorescence signals indicative of robust growth (fluorescence intensity range:  $116 \pm 3.2$ – $110 \pm 3.3$ , arbitrary units, AU, mean  $\pm$  SE;  $p = 0.18$ ,  $t$  test, Figure 1A). In contrast, yeast bearing a plasmid for a nonfunctional channel<sup>26</sup> showed little growth in potassium-limited conditions, 0–2 mM KCl ( $30 \pm 0.1$ – $32 \pm 0.2$  AU) and only propagated with 50 mM KCl ( $87 \pm 1.5$  AU, Figure 1A). Yeast expressing K<sub>2p</sub>2.1 (TREK-1) that were grown in potassium-limited conditions, 0–2 mM KCl, had resazurin fluorescence signals that were substantially larger than the negative control and that indicated rescue by a functional channel ( $67 \pm 0.5$  vs  $30 \pm 0.1$  AU, respectively,  $p < 0.001$ ,  $t$  test, Figure 1A). Interestingly, in nonlimiting 50 mM KCl media, K<sub>2p</sub>2.1 (TREK-1)-expressing cells exhibited reduced growth compared to potassium-limited conditions, 1.2 or 2 mM KCl, ( $84 \pm 1.2$  AU,  $p < 0.001$  vs 1.2 or 2 mM KCl,  $t$  test) that was comparable to that of the negative control (Figure 1A). This effect was not observed for Trk1p (Figure 1A) and is reminiscent of prior studies where activation of a heterologously expressed potassium channel caused yeast growth inhibition.<sup>33</sup> Together, these experiments show that K<sub>2p</sub>2.1 (TREK-1) supports viability of SGY1528 in liquid media under potassium-limiting conditions, a result that agrees with solid media studies.<sup>22</sup> Importantly, this liquid-based, 384-well format was suited to automated plate reader analysis. Hence, we

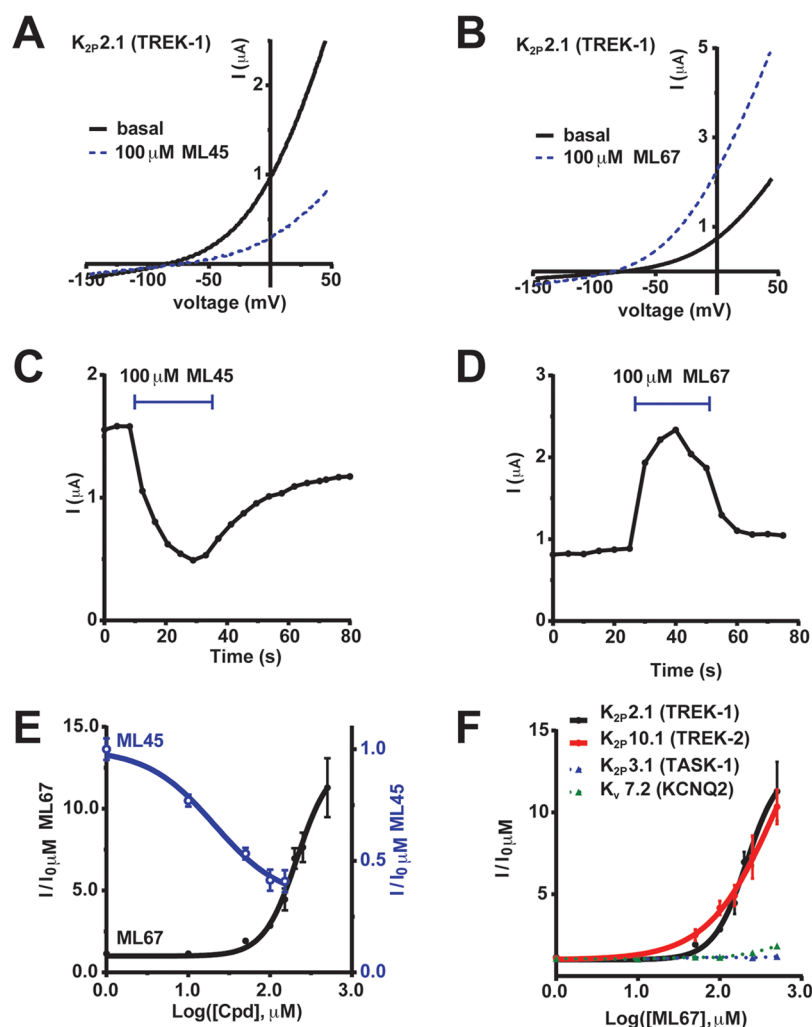


**Figure 2.** ML45 and ML67 reversibly modulate  $K_{2p}$  activity in *Xenopus* oocytes. (A, B) Exemplar two-electrode voltage clamp I–V curves for application of 100  $\mu\text{M}$  (A) ML45 or (B) ML67 measured using a  $-150$  to  $50$  mV ramp from a  $-80$  mV holding potential in  $2$  mM  $[\text{K}^+]_o$ . (C, D) Exemplar  $K_{2p2.1}$  (TREK-1) responses to 100  $\mu\text{M}$  (C) ML45 or (D) ML67 measured at  $20$  mV and  $0$  mV for ML45 and ML67, respectively. (E) ML45 and ML67 dose–response for  $K_{2p2.1}$  (TREK-1). “Cpd” denotes tested compound. Data were normalized to basal activity and fit with the Hill equation. (F) Dose–responses measured by two-electrode voltage clamp for ML67 against  $K_{2p2.1}$  (TREK-1), black;  $K_{2p10.1}$  (TREK-2), red;  $K_{2p3.1}$  (TASK-1), green; and  $\text{Kv}7.2$  (KCNQ2), blue. Error bars show SE,  $n \geq 6$ ,  $N \geq 2$ , where  $n$  and  $N$  is the number of oocytes or independent oocyte batches, respectively.

next sought to define conditions suitable for a HTS screen for regulators of  $K_{2p2.1}$  (TREK-1) activity.

Resazurin assessment of the effects of 1% dimethyl sulfoxide (DMSO), the test compound carrier, and 0.1% sodium dodecyl sulfate, SDS, a growth inhibition control, established two important assay properties. First, DMSO did not inhibit growth of  $K_{2p2.1}$  (TREK-1)-expressing yeast in potassium-limiting conditions ( $2$  mM KCl) where the active channel is required for survival, whereas SDS was lethal. Second, measurement of the  $Z'$  value, a widely used HTS assay metric for determining the separation between negative and positive controls where  $Z' > 0.5$  indicates a robust screen,<sup>34</sup> yielded a favorable value,  $Z' = 0.76$  (Figure 1B). Hence, we proceeded with a screening campaign to identify candidate  $K_{2p2.1}$  (TREK-1) modulators.

We screened a library of 106,281 small molecules at  $10$   $\mu\text{M}$  each for their ability to inhibit growth of  $K_{2p2.1}$  (TREK-1)-expressing yeast (Figure 1B, Supplementary Figure S1, Supplementary Table S1). Each plate included wells for 1% DMSO and 0.1% SDS, which served as the respective 0% and 100% growth inhibition controls for calculating the degree of

compound-induced growth inhibition (Supplementary Figure S1). From the initial screen, we chose 320 compounds for further evaluation from the set that inhibited growth in the range of 44–92% (a range representing  $1.25$ – $3\sigma$  above the mean inhibition from the screen and including an upper limit chosen to reduce toxic compound identification, cf. Supplementary Methods). To distinguish generally toxic compounds in this set from those that caused  $K_{2p2.1}$  (TREK-1)-specific effects, we tested each of the 320 compounds over a range of  $0.4$ – $50$   $\mu\text{M}$  in dose–response screen against yeast expressing  $K_{2p2.1}$  (TREK-1) or Trk1p (Figure 1C,D). These tests identified 81 compounds having at least a 2-fold difference in the apparent  $\text{IC}_{50}$  required to prevent growth  $K_{2p2.1}$  (TREK-1) versus Trk1p expressing yeast, e.g., ML45 and ML67 (Figure 1C,D). From these  $K_{2p2.1}$  (TREK-1)-specific compounds, we were able to purchase 61 in quantities sufficient for electrophysiological analysis.

Twenty-five of the 61 candidate compounds were soluble in aqueous solution at a concentration range suited for initial electrophysiological assays ( $100$ – $750$   $\mu\text{M}$ ) and were tested by

Table 1. Effects of Activator Compounds on  $K_{2p}$  Channels and Mutants<sup>a</sup>

channel	compound	EC <sub>50</sub> ( $\mu$ M)	H <sup>b</sup>	E <sub>max</sub> (fold)
K <sub>2p</sub> 2.1 (TREK-1)	ML67	213.0 $\pm$ 1.2	2.1 $\pm$ 0.6	~11
	ML67-2	ND	na	1.3 $\pm$ 0.1 at 500 $\mu$ M
	ML67-13	177.4 $\pm$ 1.1	2.2 $\pm$ 0.5	~20
	ML67-15	ND		4.7 $\pm$ 0.9 at 200 $\mu$ M
	ML67-17	162.2 $\pm$ 1.2	2.4 $\pm$ 1.1	~14
	ML67-18	124.8 $\pm$ 1.2	1.2 $\pm$ 0.2	~18
	ML67-29	250.6 $\pm$ 2.0	1.9 $\pm$ 1.4	~18
	ML67-33	36.3 $\pm$ 1.0	3.6 $\pm$ 0.4	11.1 $\pm$ 0.4
K <sub>2p</sub> 2.1 (TREK-1) G137I	ML67-137	>40	na	9.2 $\pm$ 1.4 <sup>d</sup>
	ML67-33	ND	na	0.9 $\pm$ 0.1 at 150 $\mu$ M
K <sub>2p</sub> 2.1 (TREK-1) W275S	ML67-33	21.8 $\pm$ 1.3	1.6 $\pm$ 0.7	5.1 $\pm$ 0.6
K <sub>2p</sub> 2.1 (TREK-1)-3G	ML67-33	49.4 $\pm$ 1.1	2.2 $\pm$ 0.4	12.9 $\pm$ 1.0
K <sub>2p</sub> 10.1 (TREK-2)	ML67	~250	1.0 $\pm$ 0.4	10.1 $\pm$ 1.1 at 500 $\mu$ M
	ML67-33	30.2 $\pm$ 1.4	1.6 $\pm$ 0.6	11.4 $\pm$ 1.8
K <sub>2p</sub> 4.1 (TRAAK)	ML67-33	27.3 $\pm$ 1.2	1.8 $\pm$ 0.4	14.7 $\pm$ 1.1 <sup>d</sup>
K <sub>2p</sub> 9.1 (TASK-3)	ML67-33	ND	na	2.1 $\pm$ 0.4 at 150 $\mu$ M
K <sub>2p</sub> 5.1 (TASK-2)	ML67-33	ND	na	1.7 $\pm$ 0.3 <sup>d</sup>
K <sub>2p</sub> 3.1 (TASK-1)	ML67	ND	na	1.2 $\pm$ 0.0 at 500 $\mu$ M
	ML67-33	ND	na	1.1 $\pm$ 0.1 <sup>d</sup>
K <sub>2p</sub> 18.1 (TRESK)	ML67-33	ND	na	0.9 $\pm$ 0.1 <sup>d</sup>
Kv7.2 (KCNQ2)	ML67	ND	na	1.8 $\pm$ 0.0 at 500 $\mu$ M

<sup>a</sup>ND = not determined; na = not applicable. <sup>b</sup>C Cooperativity coefficient from the Hill equation. <sup>c</sup>Measurements from HEK293 cells. <sup>d</sup>Value determined at 100  $\mu$ M compound.

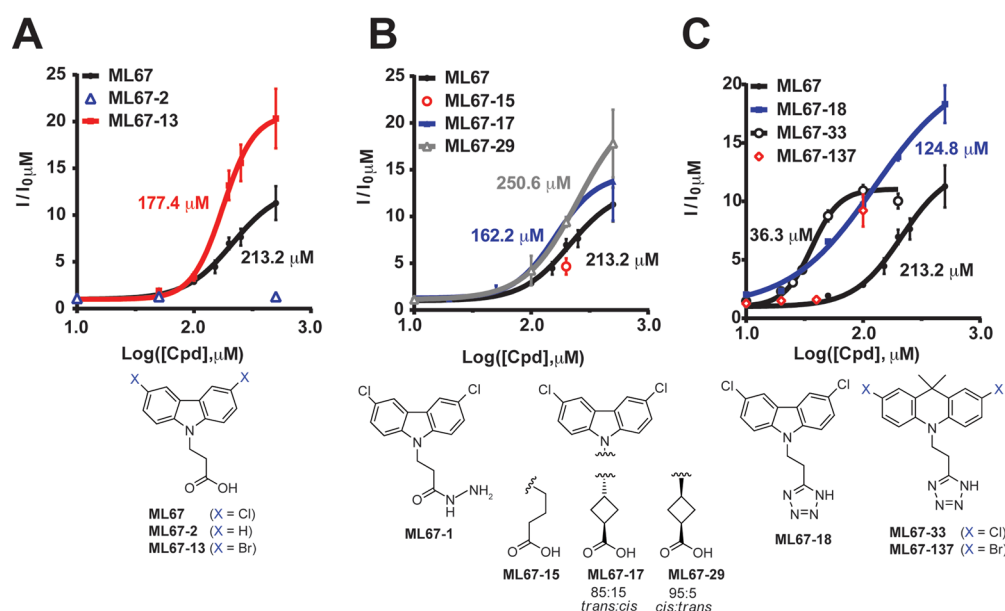


**Figure 3.** Studies to improve ML67 potency. Effects of changes to ML67 (A) halogen positions, (B) linker region, and (C) acidic group measured against K<sub>2p</sub>2.1 (TREK-1) by a  $-150$  to  $50$  mV ramp from a  $-80$  mV holding potential using two-electrode voltage clamp in *Xenopus* oocytes in  $2$  mM  $[K^+]_o$ . "Cpd" denotes tested compound. Data (mean  $\pm$  SE,  $n \geq 6$ ,  $N \geq 2$ ) from  $0$  mV were normalized to basal activity and fitted to the Hill equation. EC<sub>50</sub> values are ML67-13,  $177.4 \pm 1.1$   $\mu$ M; ML67-17,  $162.2 \pm 1.2$   $\mu$ M; ML67-29,  $250.6 \pm 2.0$   $\mu$ M; ML67-18,  $124.8 \pm 1.2$   $\mu$ M; ML67-33,  $36.3 \pm 1.0$   $\mu$ M. Error bars show SE,  $n \geq 6$  and  $N \geq 2$  except for ML67-2 and ML67-15 where  $n = 4$  and  $N = 2$ . Compound structures are shown.

two-electrode voltage clamp for activity against K<sub>2p</sub>2.1 (TREK-1) expressed in *Xenopus* oocytes. Electrophysiological characterization identified five compounds that affected K<sub>2p</sub>2.1 (TREK-1). Two acted as inhibitors: a pyrimidine (ML45) and a thiophene (ML58) (Supplementary Figure S2). Three activated the channel: a thiazolidine (ML12), an amantadine derivative (ML42), and a carbazole (ML67) (Supplementary Figure S3). Dose–response studies showed that ML45 reversibly inhibited

K<sub>2p</sub>2.1 (TREK-1) by  $\sim 70\%$  at the highest concentration tested (IC<sub>50</sub>  $\sim 21$   $\mu$ M, Figure 2A,C,E). In contrast, ML67 reversibly activated K<sub>2p</sub>2.1 (TREK-1), increasing currents by up to  $\sim 11$ -fold (EC<sub>50</sub>  $213.0 \pm 1.2$   $\mu$ M, Figure 2 B,D,E and Table 1). Because K<sub>2p</sub>2.1 (TREK-1) activators could provide a path to novel anesthetics, analgesics, and neuroprotectants<sup>3</sup> and because there were readily available derivatives, we chose to focus on the activator ML67.

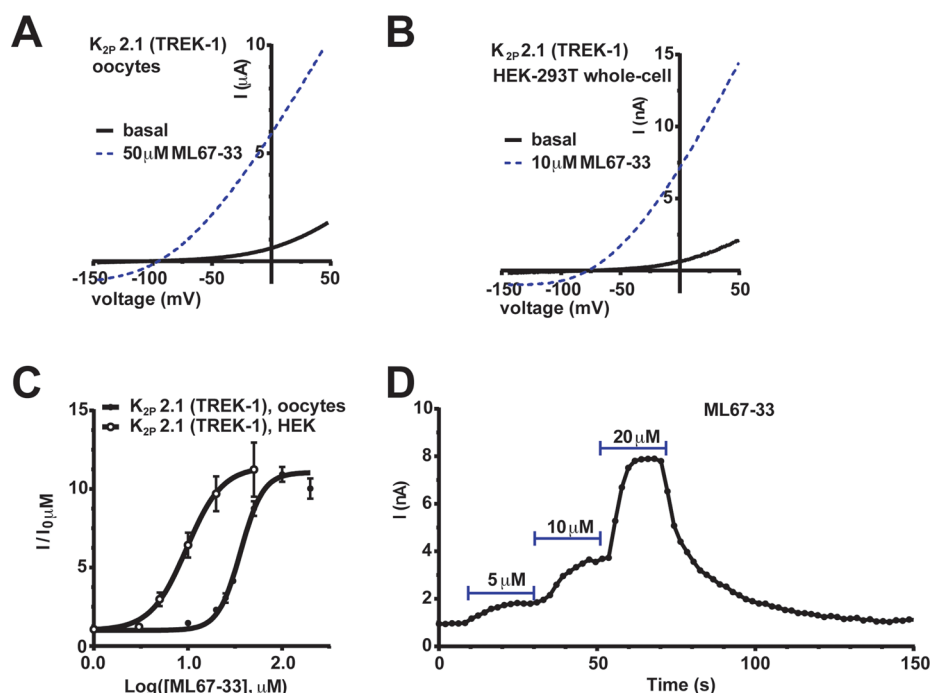


**Figure 4.** ML67-33 reversibly activates K<sub>2p</sub>2.1 (TREK-1) independent of expression system. (A, B) Exemplar I–V curves showing the effect of ML67-33 on K<sub>2p</sub>2.1 (TREK-1) activity in (A) *Xenopus* oocytes (two-electrode voltage clamp) or (B) HEK-293T cells (whole cell patch clamp). In both, the external solution contained 2 mM [K<sup>+</sup>]<sub>o</sub>, pH 7.4. Currents were elicited by a –150 to 50 mV voltage ramp from a –80 mV (oocytes) or –40 mV (HEK-293T) holding potential. (C) Quantification of the effect of ML67-33 on the indicated channels. Data (mean ± SE,  $n \geq 6$ ,  $N \geq 2$ ) were normalized to basal channel activity and fit with the Hill equation.  $EC_{50}$   $36.3 \pm 1.0 \mu\text{M}$ ,  $9.7 \pm 1.2 \mu\text{M}$  and  $E_{\text{max}}$  at  $100 \mu\text{M}$   $11.1 \pm 0.4$ ,  $11.4 \pm 1.1$  for oocytes and HEK cells, respectively. (D) Exemplar reversible activation of K<sub>2p</sub>2.1 (TREK-1) by ML67-33 measured at 0 mV in HEK-293T cells.

We first addressed whether ML67 was a selective or general potassium channel opener. Two electrode voltage clamp studies showed that ML67 activated the closest K<sub>2p</sub>2.1 (TREK-1) homologue (Supplementary Figure S4) K<sub>2p</sub>10.1 (TREK-2) ( $EC_{50} \sim 250 \mu\text{M}$ ) but not the more distantly related K<sub>2p</sub>3.1 (TASK-1) (Figure 2F). Further, ML67 had no effect on the voltage-gated potassium channel Kv7.2 (KCNQ2) (Figure 2F) for which small molecule openers have been described.<sup>35</sup> Having established that ML67 had some selectivity among diverse potassium channels, we sought to characterize its structure–activity relationships with respect to channel activation and improve upon its properties.

**ML67 Derivatives Improve Potency for K<sub>2p</sub>2.1 (TREK-1).** Investigation of substitution on the ML67 central carbazole ring showed that the hydrophobic halogen atoms were important. Removal of the chloro substituents at the carbazole ring 3- and 6-positions abolished activity (ML67-2, Figure 3A, Table 1), whereas the 3,6-dibromo congener ML67-13 showed a slightly increased potency ( $EC_{50}$   $177.4 \pm 1.1 \mu\text{M}$ ) and a dramatically improved maximum response (efficacy) ( $E_{\text{max}} \sim 20$  fold) (Figure 3A, Table 1). Thus, hydrophobic groups at the 3- and 6-positions are vital for function in the ML67 series.

With regard to the *N*-alkyl side chain, we found that the carboxylate function was critical for activity, as the nitrile congener (ML67-1) (Figure 3B) showed no activity, even at  $500 \mu\text{M}$ . Extending the alkyl chain by one methylene (ML67-15) did not improve activity (Figure 3B). Rigidification of the alkyl chain by a cyclobutane group (ML67-17 and ML67-29, *cis:trans* stereoisomer ratio 15:85 and 95:5, respectively) had a favorable effect compared to ML67-15:  $EC_{50}$   $162.2 \pm 1.2$  and  $250 \pm 2 \mu\text{M}$  for ML67-17 and ML67-29, respectively (Figure 3B, Table 1). The relative positioning of carbazole ring and

carboxylate function will be quite different in these two stereoisomeric analogues. Therefore, their similar  $EC_{50}$  values suggest that precise positioning of the carboxylate is not essential. Consistent with this notion, replacement of the carboxylate with a bioisosteric and anionic tetrazole ring (ML67-18) was well tolerated and improved potency almost 2-fold ( $EC_{50}$   $124.8 \pm 1.2$ ,  $E_{\text{max}} \sim 18$ -fold, Figure 3C, Table 1). Having established the importance of the halogen substituents and anionic tetrazole, we turned to modification of the core tricyclic ring system.

We explored a number of halogenated tricyclic ring systems bearing anionic side chains. These yielded varying degrees of success at improving K<sub>2p</sub>2.1 (TREK-1) activation. The most effective had substitution of the carbazole tricycle for 9,9-dimethyl-9,10-dihydroacridine. Analogue ML67-33 exhibited a 5-fold improved potency compared to that of ML67-18, but somewhat reduced efficacy ( $EC_{50}$   $36.3 \pm 1.0 \mu\text{M}$ ,  $E_{\text{max}}$   $11.1 \pm 0.4$  fold, Figure 3C, Table 1). The corresponding dibromo congener ML67-137 was no more potent than ML67-18 (Figure 3C, Table 1). As ML67-33 (2,7-dichloro-9,9-dimethyl-10-[2-(1*H*-tetrazol-5-yl)-ethyl]-9,10-dihydro-acridine) was the most potent compound and had favorable solubility properties ( $\text{clog } P = 4.84$ ,  $\text{clog } D = 3.29$  at pH 7.4, Supplementary Table S2), we pursued a series of experiments designed to test its mechanism of action.

#### ML67-33 Activates the K<sub>2p</sub>2.1 (TREK-1) C-Type Gate.

We examined how ML67-33 affected K<sub>2p</sub>2.1 (TREK-1) expressed in two widely used experimental systems, *Xenopus* oocytes and mammalian HEK-293T cells. ML67-33 had similar potencies and efficacies on K<sub>2p</sub>2.1 (TREK-1) expressed in both systems (Figure 4A and B) ( $EC_{50}$   $36.3 \pm 1.1 \mu\text{M}$  and  $9.7 \pm 1.2 \mu\text{M}$  and  $E_{\text{max}}$   $11.1 \pm 0.4$  and  $11.4 \pm 1.1$  for oocytes and HEK

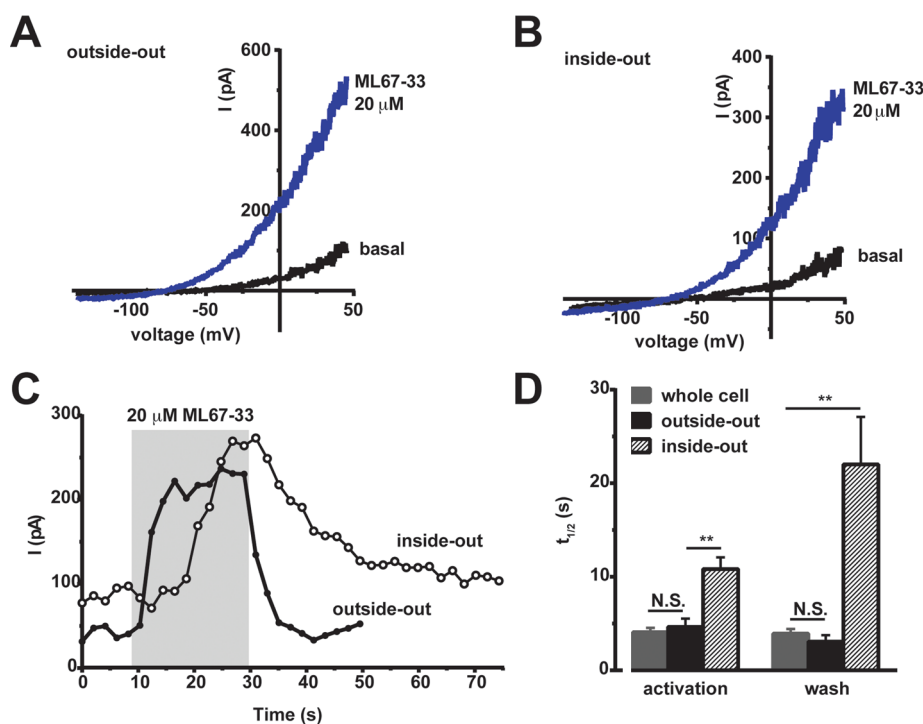


**Figure 5.** ML67-33 activates  $K_{2p2.1}$  (TREK-1) in excised membrane patches. (A, B) Exemplar I–V curves showing ML67-33 effects on  $K_{2p2.1}$  (TREK-1) in (A) outside-out and (B) inside-out excised patches from HEK-293T cells. Currents were elicited by a  $-100$  to  $50$  mV ramp from a  $-40$  mV holding potential. (C) Exemplar responses to ML67-33 measured at  $0$  mV in the indicated configurations. Gray indicates presence of  $20 \mu\text{M}$  ML67-33. (D) Time to half-maximal activation following ML67-33 application and recovery from activation (wash) following ML67-33 removal, measured in HEK-293T cells at  $0$  mV. Error bars: mean  $\pm$  SE  $n \geq 6$ ,  $N \geq 2$ . \*\*  $p \leq 0.01$ ; N.S. indicates not significant ( $p \geq 0.05$ ) as determined by  $t$  test.

cells, respectively, Figure 4C, Table 1), demonstrating that the compound acts independently of cellular context (Figure 4A–C). Further, the effects of ML-67-33 were fast, occurring within seconds (half-maximal activation time,  $4.1 \pm 0.5$  s, mean  $\pm$  SE,  $n = 7$ ,  $N = 2$ ) and were reversible (Figure 4D). ML67-33 application to excised membrane patched from HEK cells expressing  $K_{2p2.1}$  (TREK-1) showed that ML67-33 activated  $K_{2p2.1}$  (TREK-1) in both the outside-out (Figure 5A) and inside-out (Figure 5B) configurations. The effectiveness in both contexts strongly suggests that ML67-33 acts directly on the channel and does not require soluble cytosolic factors. The times of half-maximal activation and return to baseline following compound washout ( $t_{1/2\text{act}}$  and  $t_{1/2\text{wash}}$ , respectively) in the outside-out configuration were indistinguishable from those measured in the whole-cell configuration ( $t_{1/2\text{act}}$ :  $t_{1/2\text{wash}}$  mean  $\pm$  SE,  $4.1 \pm 0.5$  s:  $3.9 \pm 0.5$  s and  $4.6 \pm 0.9$  s;  $3.1 \pm 0.7$  s for whole-cell and outside-out, respectively, Figure 5C and D). Both  $t_{1/2}$  values slowed substantially when the compound was applied to the inside-out configuration. Notably, there was a larger effect on washout from inside-out patches ( $t_{1/2\text{act}}$ :  $t_{1/2\text{wash}}$   $10.8 \pm 1.3$  s:  $22.0 \pm 5.1$  s, Figure 5C and D). Taken together, these data indicate that although ML67-33 appears to be membrane-permeable, its site of action on  $K_{2p2.1}$  (TREK-1) is more readily accessible from the extracellular side.

A selectivity filter-based C-type-like gate mediates  $K_{2p2.1}$  (TREK-1) activation from diverse inputs that include basic extracellular pH,<sup>22,36</sup> intracellular acidosis,<sup>23</sup> temperature,<sup>22</sup> mechanical force,<sup>22</sup> and intracellular C-terminal domain, Ct, phosphorylation.<sup>21</sup> The C-type gate active conformation can be stabilized by high concentrations of extracellular potassium,  $[\text{K}^+]_o$ ,<sup>21–23,36</sup> or by mutations in the P1 pore helix, G137I,<sup>21</sup> or

the M4 transmembrane helix, W275S<sup>22</sup> (Figure 6A). We tested how each affected the response to ML67-33. The data show that all three manipulations reduced the response of  $K_{2p2.1}$  (TREK-1) to ML67-33 (Figure 6B–G). Indeed, the change causing the most potent C-type gate stabilization, G137I,<sup>21</sup> made the channels completely resistant to ML67-33 activation. In contrast, use of a triple glycine mutation,  $K_{2p2.1}$ -3G<sup>21</sup> (Figure 6A) that uncouples the pore from Ct, which acts as a sensor for temperature<sup>8,21,22</sup> and mechanical stimulation,<sup>9,22</sup> resulted in channels that could be readily activated by ML67-33. In this case, both the ML67-33 potency and efficacy were similar to that of wild-type channels ( $EC_{50}$   $49.4 \pm 0.1 \mu\text{M}$ ,  $E_{\text{max}}$   $12.9 \pm 1.0$ , Figure 6F and G). The observation that activation of the C-type gate renders the channels resistant to ML67-33 whereas loss of coupling to Ct does not affect ML67-33 activation indicates that ML67-33 acts directly on the components comprising the C-type gate. Ct is central to  $K_{2p2.1}$  (TREK-1) activation by the two most effective activators previously reported, chloroform<sup>4,9</sup> and arachidonic acid,<sup>4,9</sup> and is crucial for channel inhibition by fluoxetine (Prozac).<sup>20</sup> The lack of involvement of Ct in ML67-33 activation together with evidence for the direct action of ML67-33 on the C-type gate indicates that ML67-33 activates the channel by a novel mechanism (Figure 6H).

**ML67-33 Activates Temperature- and Mechano-Sensitive  $K_{2p}$  Channels.** To examine the ML67-33 specificity within the  $K_{2p}$  family, we used heterologous expression in *Xenopus* oocytes of representatives from different  $K_{2p}$  subtypes<sup>6</sup> (Supplementary Figure S4). These included the two temperature- and mechano-sensitive  $K_{2p}$ s most closely related to  $K_{2p2.1}$  (TREK-1),  $K_{2p10.1}$  (TREK-2) and  $K_{2p4.1}$  (TRAAK); a

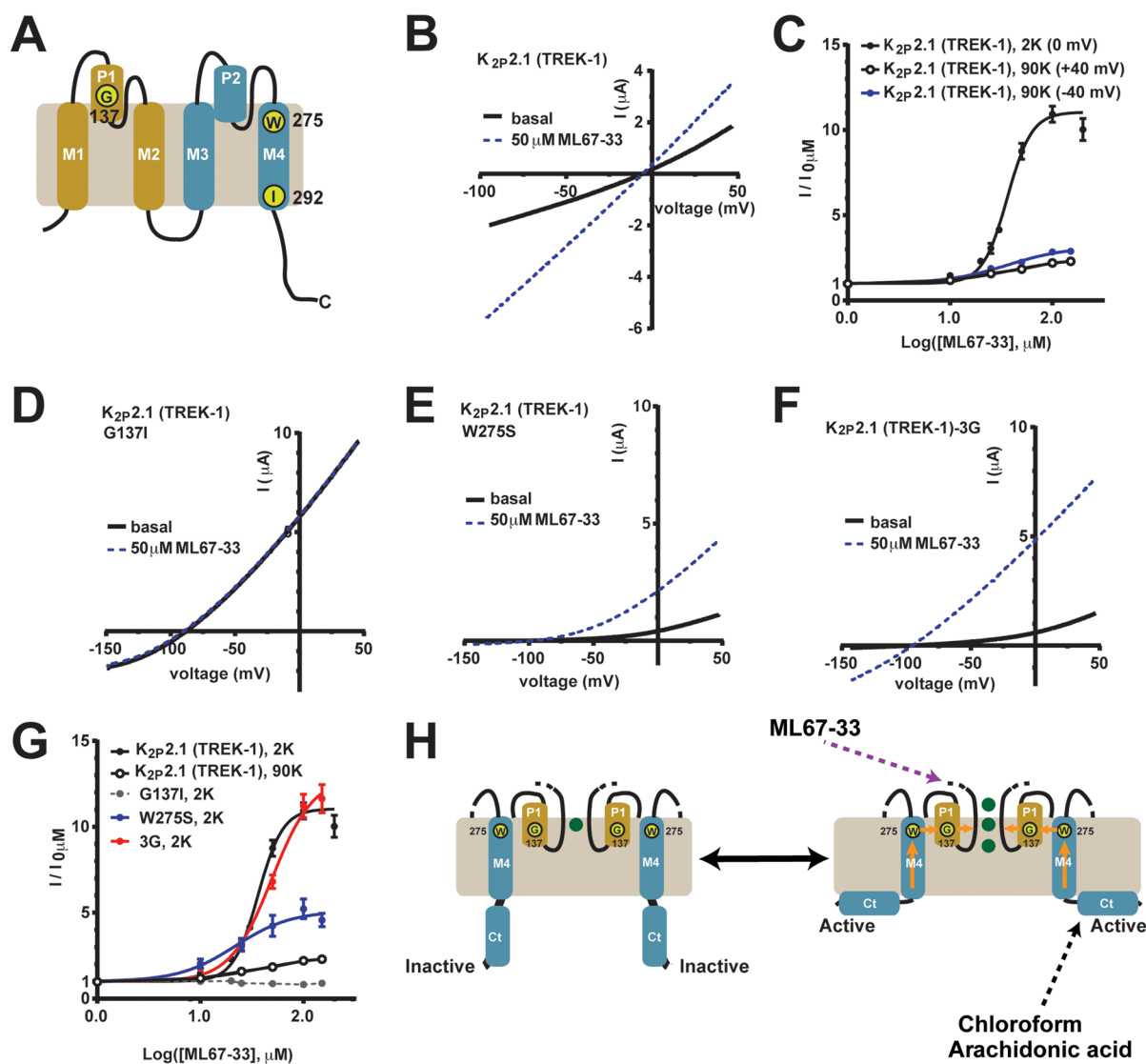


**Figure 6.** ML67-33 activates the  $K_{2p2.1}$  (TREK-1) extracellular C-type gate. (A)  $K_{2p2.1}$  (TREK-1) subunit cartoon diagram. Key residue positions, transmembrane segments (M1–M4), and pore helices (P1 and P2) are indicated. First and second pore-forming regions are tan and blue, respectively. (B–G) Exemplar two-electrode voltage clamp I–V curves in *Xenopus* oocytes and dose response curves showing ML67-33 responses in channels having perturbed gating elements. (B) C-type gate stabilization by 90 mM  $[K^+]_o$ . (C) ML67-33 dose response at +40 and –40 mV in 90 mM  $[K^+]_o$  (90K) and 0 mV in 2 mM  $[K^+]_o$  (2K). (D, E) C-type gate stabilization by (D) G137I and (E) W275S. (F) Uncoupling Ct from the pore by the  $K_{2p2.1}$  (TREK-1)-3G mutant. (G) ML67-33 dose responses for the indicated channels at +40 mV (90K) or 0 mV (2K), normalized to basal channel activity and fit with the Hill equation. Error bars indicate SE,  $n \geq 6$ ,  $N \geq 2$ . (H) Model of  $K_{2p2.1}$  (TREK-1) activation after ref 21. Green spheres indicate potassium ions. Positions of Gly137 and Trp275 are indicated. Orange arrows indicate pathway for coupling Ct activation to the C-type gate. Elements involved in activation by ML67-33, chloroform,<sup>9</sup> and arachidonic acid<sup>9</sup> are indicated. I–V curves were measured in (B) 90 mM  $[K^+]_o$  or (D–F) 2 mM  $[K^+]_o$ . Currents were elicited by a –100 to 50 mV ramp from a 0 mV holding potential (90K) or by a –150 to 50 mV ramp, from a –80 mV holding potential (2K).

representative from the neighboring subgroup, the *TALK* subgroup,  $K_{2p5.1}$  (TASK-2); and representatives from two divergent branches of the  $K_{2p}$  family, the *TASK* subgroup,  $K_{2p3.1}$  (TASK-1) and  $K_{2p9.1}$  (TASK-3); and  $K_{2p18.1}$  (TRESK). ML67-33 exhibited substantial activation of  $K_{2p10.1}$  (TREK-2) (Figure 7A, Supplementary Figure S5A) ( $EC_{50}$   $30.2 \pm 1.4$ ,  $E_{max}$   $11.4 \pm 1.8$  fold, Table 1) and  $K_{2p4.1}$  (TRAAK) (Figure 7B, Supplementary Figure S5B) ( $EC_{50}$   $27.3 \pm 1.18$   $\mu$ M,  $E_{max}$   $14.7 \pm 1.12$  fold, Table 1). In stark contrast, ML67-33 showed little or no activity against channels from the *TALK* group,  $K_{2p5.1}$  (TASK-2) (Figure 7C and G, Table 1); *TASK* group,  $K_{2p3.1}$  (TASK-1) (Figure 7D and G, Table 1) and  $K_{2p9.1}$  (TASK-3) (Figure 7E and G, Table 1); and  $K_{2p18.1}$

(TRESK) (Figure 7F and G, Table 1) even when applied at 100  $\mu$ M, a concentration at which  $K_{2p2.1}$  (TREK-1) shows a maximal response. Similar to the parent compound ML67 (Figure 2F), ML67-33 at 100  $\mu$ M showed no effect on Kv7.2 (KCNQ2) (Supplementary Figure S6). Together, these data establish that ML67-33 is a selective activator of channels from the  $K_{2p2.1}$  (TREK-1) subfamily of temperature- and mechano-sensitive channels.

**Discussion.**  $K_{2p}$  channels are the most diverse potassium channel class<sup>37</sup> and function in both excitable and nonexcitable cells.<sup>1</sup> The fact that this channel family responds poorly to classic potassium channel blockers<sup>4</sup> and remains largely pharmacologically orphaned<sup>3,4</sup> limits the ability to probe its

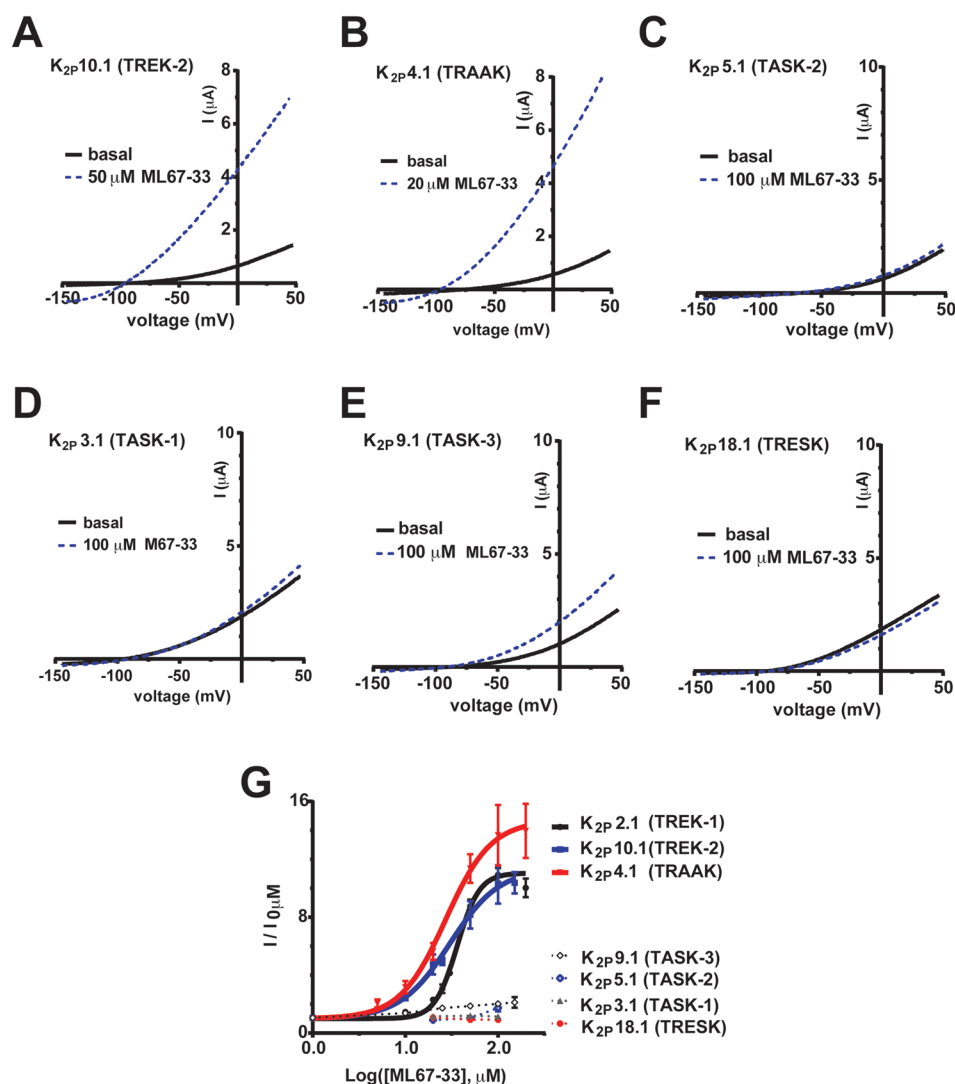


**Figure 7.** ML67-33 is a selective activator of temperature- and mechanosensitive  $K_{2P}$  channels. (A–F) Exemplar I–V curves showing ML67-33 effects on (A)  $K_{2P}10.1$  (TREK-2), (B)  $K_{2P}4.1$  (TRAAK), (C)  $K_{2P}5.1$  (TASK-2), (D)  $K_{2P}3.1$  (TASK-1), (E)  $K_{2P}9.1$  (TASK-3), and (F)  $K_{2P}18.1$  (TRESK) measured in *Xenopus* oocytes using a  $-150$  to  $50$  mV ramp from a  $-80$  mV holding potential in  $2$  mM  $[K^+]_o$ . (G) ML67-33 dose responses for the indicated channels. Data (mean  $\pm$  SE,  $n \geq 6$ ,  $N \geq 2$ ) were normalized to basal activity and fit with the Hill equation.  $EC_{50}$  values:  $K_{2P}2.1$  (TREK-1)  $36.3 \pm 1.0$   $\mu$ M,  $K_{2P}10.1$  (TREK-2)  $30.2 \pm 1.4$   $\mu$ M, and  $K_{2P}4.1$  (TRAAK)  $27.3 \pm 1.2$   $\mu$ M.  $E_{max}$  values at  $100$   $\mu$ M are  $K_{2P}2.1$  (TREK-1)  $11.1 \pm 0.4$ ,  $K_{2P}10.1$  (TREK-2)  $11.4 \pm 1.8$ ,  $K_{2P}4.1$  (TRAAK)  $14.7 \pm 1.1$ ,  $K_{2P}5.1$  (TASK-2)  $2.0 \pm 0.1$ ,  $K_{2P}9.1$  (TASK-3)  $1.7 \pm 0.3$ ,  $K_{2P}3.1$  (TASK-1)  $1.1 \pm 0.0$ ,  $K_{2P}18.1$  (TRESK)  $0.9 \pm 0.1$ . Error bars indicate SE,  $n \geq 6$ ,  $N \geq 2$ .

function. Additionally, because  $K_{2P}$ s produce voltage-independent leak current, they present difficult targets for modulator discovery by conventional electrophysiological screening techniques. Our studies demonstrate that it is possible to use a solution-based yeast screening platform built upon rescue of potassium uptake by a functional  $K_{2P}$  channel to identify both inhibitors and activators of  $K_{2P}$ s. This assay provides a substantial advantage in terms of scalability and quantification over solid-based media assays used previously to screen small libraries against other potassium channels.<sup>28,29</sup>

We identified a set of novel  $K_{2P}2.1$  (TREK-1) inhibitors and activators in a single screening campaign covering 106,281 compounds. Because all of the identified compounds inhibited  $K_{2P}2.1$  (TREK-1)-dependent yeast growth, our discovery of molecules that proved to be activators was unexpected. Examination of the potassium dependency of yeast rescue in solution showed that, unlike the potassium transporter Trk1p,  $K_{2P}2.1$  (TREK-1) conferred a bell-shaped dependence on

growth rescue as a function of potassium (Figure 1A), an effect not seen previously in solid media assays.<sup>22</sup> Prior identification of gain-of-function mutants of the yeast channel YKC1 (TOK1) has shown that hyperactive potassium channels can negatively impact yeast growth.<sup>33</sup> Although the exact mechanism by which  $K_{2P}2.1$  (TREK-1) hyper-activation causes growth inhibition remains unclear, the results from the YKC1 (TOK1) studies suggest a rationale for why our high-throughput screen identified inhibitors and activators of  $K_{2P}2.1$  (TREK-1) in a single screening campaign. Because inhibitors and activators of  $K_{2P}2.1$  (TREK-1) are desirable for both physiological studies and as leads for therapeutic applications,<sup>3</sup> this unexpected benefit substantially expands the potential of this assay to identify  $K_{2P}$  modulators from diverse chemical libraries.

The two inhibitors and three activators that we identified produced fast, reversible changes in  $K_{2P}2.1$  (TREK-1) function that occurred within seconds of compound application and



removal (Supplementary Figures S2 and S3). This is notable because the yeast HTS assay time scale is hours and could favor the identification of slow-acting compounds that have indirect effects on channel function by affecting factors such as channel biogenesis, assembly, or trafficking. Although such compounds could in principle be identified, the fact that we found diverse compounds that appear to act directly and immediately on the channel indicates that there is no strong bias for slow-acting effectors and underscores the potential of this assay as a discovery platform for fast-acting  $K_{2p}$  channel modulators.

By combining biophysical characterization and chemical synthesis, we improved upon the properties of a lead activator, ML67 (Figure 3, Table 1), to create a dihydroacridine derivative that reversibly activated  $K_{2p2.1}$  (TREK-1) (Figure 4) with an  $EC_{50}$  in the low-micromolar range and an  $E_{max}$  of  $\sim 11$  (Table 1). The observation that ML67-33 activates  $K_{2p2.1}$  (TREK-1) in excised membrane patches (Figure 5) demonstrates that the compound does not act by perturbing channel trafficking or via a mechanism that involves cytosolic proteins and suggests that ML67-33 acts directly on the channel.

Diverse gating signals that include protons, temperature, mechanical force, and phosphorylation control  $K_{2p2.1}$  (TREK-1) function. Although many of these are sensed by the intracellular cytoplasmic domain, Ct,<sup>8,21,38–40</sup> their actions converge on a common C-type selectivity filter-based gate located on the extracellular side of the membrane.<sup>21–23,36,41</sup> A variety of manipulations that stabilize this C-type gate, such as high concentrations of extracellular potassium<sup>36</sup> and mutations in two elements central to C-type gate activation, the P1 pore helix and M4 transmembrane helix,<sup>22</sup> reduced or eliminated the activating effects of ML67-33 (Figure 6B–E and G). By contrast, decoupling Ct from the C-type gate failed to affect channel sensitivity to ML67-33 (Figure 6F and G). This result eliminates this region as the target of ML67-33 action and is striking because in addition to sensing physiological inputs, Ct is thought to be central to  $K_{2p2.1}$  (TREK-1) modulation by compounds such as chloroform,<sup>9</sup> arachidonic acid,<sup>9</sup> and fluoxetine (Prozac).<sup>20</sup> Further, we found that ML67-33 acts quickly and reversibly when applied to channels in whole cells and outside-out patches but displays slower on and off rates when applied to channels in the inside-out patch configuration (Figure 5C and D). Together, these observations strongly support the idea that ML67-33 acts directly on the extracellular C-type gate and indicate that ML67-33 has a mechanism that is different from other  $K_{2p2.1}$  (TREK-1) modulators and that targets the core machinery that controls channel gating (Figure 6H).

ML67-33 activates two, closely related temperature- and mechano-sensitive  $K_{2p}$  channels,  $K_{2p10.1}$  (TREK-2) and  $K_{2p4.1}$  (TRAAK), with an  $EC_{50}$  in the low-micromolar range (Figure 7, Table 1). In contrast, ML67-33 was ineffective against more the distantly related members of the  $K_{2p}$  family  $K_{2p5.1}$  (TASK-2),  $K_{2p3.1}$  (TASK-1),  $K_{2p9.1}$  (TASK-3), and  $K_{2p18.1}$  (TRESK) and against the voltage-gated channel Kv7.2 (KCNQ2) (Figure 7, Supplementary Figure S6). The C-type, selectivity filter-based gating mechanism acts in channels that respond to ML67-33,  $K_{2p2.1}$  (TREK-1),<sup>22,23,36</sup> and  $K_{2p10.1}$  (TREK-2),<sup>22</sup> as well as those that were resistant to the compound,  $K_{2p3.1}$  (TASK-1)<sup>42–44</sup> and  $K_{2p5.1}$  (TASK-2).<sup>45</sup> Thus, the presence of a C-type gate is necessary but not sufficient for activation by ML67-33. Further, the selectivity profile of the compound suggests that key targets of ML67-33 action must lie in elements that are common to the  $K_{2p2.1}$  (TREK-1) subfamily.

A number of compounds modulate  $K_{2p2.1}$  (TREK-1) activity.<sup>4</sup> Many are drugs having numerous molecular targets or metabolites involved in multiple pathways such as local<sup>46,47</sup> and general<sup>9,10,17</sup> anesthetics, antidepressants,<sup>9,19</sup> neuroprotectants,<sup>18,48</sup> phospholipids,<sup>38,49</sup> protons,<sup>36,39,50</sup> and heavy metal ions.<sup>17</sup> Most of these  $K_{2p2.1}$  (TREK-1) modulators act at  $>100$   $\mu\text{M}$ , have limited effects on current amplitude,<sup>4</sup> and current enhancements of  $<2$ -fold.<sup>10,17,47,51</sup> The largest reported activations are for chloroform (5.5-fold at 1.6 mM)<sup>9</sup> and arachidonic acid (3–12-fold at 10–20  $\mu\text{M}$ ),<sup>9,47</sup> a polyunsaturated fatty acid with multiple biological functions. ML67-33 acts at a lower concentration (9.7–36.3  $\mu\text{M}$ ) and has a larger stimulatory effect ( $E_{max} \sim 11$ -fold) than most previously reported activators.<sup>4</sup> Although ML67-33 activation matches that of the most effective but unspecific activator, arachidonic acid,<sup>9,47</sup> ML67-33 stimulation of  $K_{2p2.1}$  (TREK-1) does not require Ct (Figure 6F), a channel element that is central to the action of chloroform,<sup>4,9</sup> arachidonic acid,<sup>4,9</sup> and other gating inputs.<sup>8,21,38–40</sup> Instead, our data indicate that the potent activation caused by ML67-33 involves direct action on the C-type gate that forms the core gating apparatus of the channel<sup>21–23,41</sup> (Figure 6H). These properties, together with the fact that ML67-33 acts within seconds, suggest that ML67-33 has a novel mechanism of action and focuses attention on the C-type gate for future structure-based development of  $K_{2p}$  modulators.

ML67-33 displays marked specificity within the  $K_{2p}$  group and thus should provide a key step in the development of selective regulators of the  $K_{2p2.1}$  (TREK-1) subfamily. Such compounds may afford new entry points for neuroprotective and cardioprotective molecules that could be useful for the treatment of ischemia or pain control. Finally, the demonstrated ability of our high-throughput yeast-based screening assay to identify both activators and inhibitors of  $K_{2p2.1}$  (TREK-1) suggests that this platform can be adapted to screen for regulators of other  $K_{2ps}$ . Our findings should enable new mechanistic and physiological investigations of  $K_{2p}$  activity as well as the further discovery of other  $K_{2p}$  small molecule modulators.

## METHODS

**Molecular Biology.** Murine  $K_{2p}$  channels were cloned into pGEMHE/pMO,<sup>22</sup> IRES-GFP (Invitrogen), or pYES2-MET2S (high copy 2  $\mu$ , URA3)<sup>26</sup> for expression in oocytes, HEK-293T cells, and yeast, respectively, using standard molecular biology procedures, and verified by DNA sequencing.

**Yeast, Media, Compounds, and High-Throughput Screening.** *Saccharomyces cerevisiae* strain SGY1528 was transformed with previously described plasmids.<sup>22,26</sup> Resazurin (Alamar Blue, Invitrogen) signals were quantified using an automated plate reader using 560 nm excitation/590 nm emission settings. Details are found in the Supporting Information.

Library compounds were assembled at the Small Molecule Discovery Center from commercial sources. Individual compounds were purchased or synthesized.

**Electrophysiology.** Two electrode voltage clamp was done as previously described.<sup>21,22</sup> HEK293T whole cell and patch clamp recording was done following established protocols.<sup>9</sup> Data were fit with a modified Hill equation:  $I = I_{min} + (I_{max} - I_{min}) / (1 + 10^{(\log EC_{50} - \log [C]) * H})$ ;  $I_{max}$  and  $I_{min}$  are maximal and minimal current values, respectively,  $EC_{50}$  is a half-maximal effective concentration, and  $H$  is the Hill coefficient. Detailed procedures are found in the Supporting Information.

**Statistical Analysis.** Results are mean  $\pm$  SD or SEM from at least two independent experiments (denoted as *N*). Statistical analyses used the two-tailed Student's *t* test; significance defined as  $p \leq 0.05$ .

**Chemical Synthesis.** ML67, ML67-2, and ML67-13 were obtained from commercial sources. Syntheses of ML67-33, ML67-137, ML67-18, ML67-15, ML67-17, and ML67-29 are described in Supporting Information.

## ■ ASSOCIATED CONTENT

### Supporting Information

This material is available free of charge *via* the Internet at <http://pubs.acs.org>.

## ■ AUTHOR INFORMATION

### Corresponding Author

\*E-mail: [daniel.minor@ucsf.edu](mailto:daniel.minor@ucsf.edu).

### Present Address

#Department of Cellular and Molecular Physiology Yale University School of Medicine, New Haven, CT 06510.

### Author Contributions

S.N.B. and D.L.M. conceived the study and designed the experiments. S.N.B. performed the experiments and analyzed data. S.N.B. and K.K.-H.A. performed the chemical screen. A.G.G. performed chemical synthesis. S.N.B. and K.A.C. performed molecular cloning. M.R.A. supervised the chemical screen and analyzed data. A.R.R. designed new analogues and supervised chemical synthesis. D.L.M. analyzed data and provided guidance and support throughout. S.N.B. and D.L.M. wrote the paper.

### Notes

The authors declare no competing financial interest.

## ■ ACKNOWLEDGMENTS

This work was supported by grants to D.L.M. from NIH R01-MH093603 and American Heart Association 0740019N and to S.N.B. from the Life Sciences Research Foundation. D.L.M. is an AHA Established Investigator. We thank E. Gracheva and Minor lab members for comments on the manuscript. S.N.B. is a Genentech Fellow of the Life Sciences Research Foundation.

## ■ REFERENCES

- (1) Enyedi, P., and Czirjak, G. (2010) Molecular background of leak K<sup>+</sup> currents: two-pore domain potassium channels. *Physiol. Rev.* 90, 559–605.
- (2) Lesage, F., and Barhanin, J. (2011) Molecular physiology of pH-sensitive background K(2P) channels. *Physiology* 26, 424–437.
- (3) Es-Salah-Lamoureux, Z., Steele, D. F., and Fedida, D. (2010) Research into the therapeutic roles of two-pore-domain potassium channels. *Trends Pharmacol. Sci.* 31, 587–595.
- (4) Lotshaw, D. P. (2007) Biophysical, pharmacological, and functional characteristics of cloned and native mammalian two-pore domain K<sup>+</sup> channels. *Cell Biochem. Biophys.* 47, 209–256.
- (5) Fink, M., Duprat, F., Lesage, F., Reyes, R., Romey, G., Heurteaux, C., and Lazdunski, M. (1996) Cloning, functional expression and brain localization of a novel unconventional outward rectifier K<sup>+</sup> channel. *EMBO J.* 15, 6854–6862.
- (6) Noel, J., Sandoz, G., and Lesage, F. (2011) Molecular regulations governing TREK and TRAAK channel functions. *Channels (Austin)* 5, 402–409.
- (7) Honore, E. (2007) The neuronal background K2P channels: focus on TREK1. *Nat. Rev. Neurosci.* 8, 251–261.
- (8) Maingret, F., Lauritzen, I., Patel, A. J., Heurteaux, C., Reyes, R., Lesage, F., Lazdunski, M., and Honore, E. (2000) TREK-1 is a heat-activated background K(+) channel. *EMBO J.* 19, 2483–2491.

- (9) Patel, A. J., Honore, E., Maingret, F., Lesage, F., Fink, M., Duprat, F., and Lazdunski, M. (1998) A mammalian two pore domain mechano-gated S-like K<sup>+</sup> channel. *EMBO J.* 17, 4283–4290.

- (10) Patel, A. J., Honore, E., Lesage, F., Fink, M., Romey, G., and Lazdunski, M. (1999) Inhalational anesthetics activate two-pore-domain background K<sup>+</sup> channels. *Nat. Neurosci.* 2, 422–426.

- (11) Alloui, A., Zimmermann, K., Mamet, J., Duprat, F., Noel, J., Chemin, J., Guy, N., Blondeau, N., Voilley, N., Rubat-Coudert, C., Borsotto, M., Romey, G., Heurteaux, C., Reeh, P., Eschalier, A., and Lazdunski, M. (2006) TREK-1, a K<sup>+</sup> channel involved in polymodal pain perception. *EMBO J.* 25, 2368–2376.

- (12) Noel, J., Zimmermann, K., Busserolles, J., Deval, E., Alloui, A., Diochot, S., Guy, N., Borsotto, M., Reeh, P., Eschalier, A., and Lazdunski, M. (2009) The mechano-activated K<sup>+</sup> channels TRAAK and TREK-1 control both warm and cold perception. *EMBO J.* 28, 1308–1318.

- (13) Heurteaux, C., Guy, N., Laigle, C., Blondeau, N., Duprat, F., Mazzuca, M., Lang-Lazdunski, L., Widmann, C., Zanzouri, M., Romey, G., and Lazdunski, M. (2004) TREK-1, a K<sup>+</sup> channel involved in neuroprotection and general anesthesia. *EMBO J.* 23, 2684–2695.

- (14) Heurteaux, C., Lucas, G., Guy, N., El Yacoubi, M., Thummler, S., Peng, X. D., Noble, F., Blondeau, N., Widmann, C., Borsotto, M., Gobbi, G., Vaugeois, J. M., Debonnel, G., and Lazdunski, M. (2006) Deletion of the background potassium channel TREK-1 results in a depression-resistant phenotype. *Nat. Neurosci.* 9, 1134–1141.

- (15) Solt, K., and Forman, S. A. (2007) Correlating the clinical actions and molecular mechanisms of general anesthetics. *Curr. Opin. Anaesthesiol.* 20, 300–306.

- (16) Lesage, F., Terrenoire, C., Romey, G., and Lazdunski, M. (2000) Human TREK2, a 2P domain mechano-sensitive K<sup>+</sup> channel with multiple regulations by polyunsaturated fatty acids, lysophospholipids, and Gs, Gi, and Gq protein-coupled receptors. *J. Biol. Chem.* 275, 28398–28405.

- (17) Gruss, M., Bushell, T. J., Bright, D. P., Lieb, W. R., Mathie, A., and Franks, N. P. (2004) Two-pore-domain K<sup>+</sup> channels are a novel target for the anesthetic gases xenon, nitrous oxide, and cyclopropane. *Mol. Pharmacol.* 65, 443–452.

- (18) Duprat, F., Lesage, F., Patel, A. J., Fink, M., Romey, G., and Lazdunski, M. (2000) The neuroprotective agent riluzole activates the two P domain K(+) channels TREK-1 and TRAAK. *Mol. Pharmacol.* 57, 906–912.

- (19) Kennard, L. E., Chumbley, J. R., Ranatunga, K. M., Armstrong, S. J., Veale, E. L., and Mathie, A. (2005) Inhibition of the human two-pore domain potassium channel, TREK-1, by fluoxetine and its metabolite norfluoxetine. *Br. J. Pharmacol.* 144, 821–829.

- (20) Sandoz, G., Bell, S. C., and Isacoff, E. Y. (2011) Optical probing of a dynamic membrane interaction that regulates the TREK1 channel. *Proc. Natl. Acad. Sci. U.S.A.* 108, 2605–2610.

- (21) Bagriantsev, S. N., Clark, K. A., and Minor, D. L., Jr. (2012) Metabolic and thermal stimuli control K(2P)2.1 (TREK-1) through modular sensory and gating domains. *EMBO J.* 31, 3297–3308.

- (22) Bagriantsev, S. N., Peyronnet, R., Clark, K. A., Honore, E., and Minor, D. L., Jr. (2011) Multiple modalities converge on a common gate to control K2P channel function. *EMBO J.* 30, 3594–3606.

- (23) Piechotta, P. L., Rapedius, M., Stansfeld, P. J., Bollepalli, M. K., Ehrlich, G., Andres-Enguix, I., Fritzenschaft, H., Decher, N., Sansom, M. S., Tucker, S. J., and Baukrowitz, T. (2011) The pore structure and gating mechanism of K2P channels. *EMBO J.* 30, 3607–3619.

- (24) Ko, C. H., and Gaber, R. F. (1991) TRK1 and TRK2 encode structurally related K<sup>+</sup> transporters. *Mol. Cell. Biol.* 11, 4266–4273.

- (25) Tang, W., Ruknudin, A., Yang, W., Shaw, S., Knickerbocker, A., and Kurtz, S. (1995) Functional expression of a vertebrate inwardly rectifying K<sup>+</sup> channel in yeast. *Mol. Biol. Cell* 6, 1231–1240.

- (26) Minor, D. L., Jr., Masseling, S. J., Jan, Y. N., and Jan, L. Y. (1999) Transmembrane structure of an inwardly rectifying potassium channel. *Cell* 96, 879–891.

- (27) Chatelain, F. C., Gazzarrini, S., Fujiwara, Y., Arrigoni, C., Domigan, C., Ferrara, G., Pantoja, C., Thiel, G., Moroni, A., and Minor, D. L., Jr. (2009) Selection of inhibitor-resistant viral potassium

channels identifies a selectivity filter site that affects barium and amantadine block. *PLoS One* 4, e7496.

(28) Zaks-Makhina, E., Kim, Y., Aizenman, E., and Levitan, E. S. (2004) Novel neuroprotective K<sup>+</sup> channel inhibitor identified by high-throughput screening in yeast. *Mol. Pharmacol.* 65, 214–219.

(29) Zaks-Makhina, E., Li, H., Grishin, A., Salvador-Recatala, V., and Levitan, E. S. (2009) Specific and slow inhibition of the kir2.1 K<sup>+</sup> channel by gambogic acid. *J. Biol. Chem.* 284, 15432–15438.

(30) Chatelain, F. C., Alagem, N., Xu, Q., Pancaroglu, R., Reuveny, E., and Minor, D. L., Jr. (2005) The pore helix dipole has a minor role in inward rectifier channel function. *Neuron* 47, 833–843.

(31) Nakayama, G. R., Caton, M. C., Nova, M. P., and Parandoosh, Z. (1997) Assessment of the Alamar Blue assay for cellular growth and viability in vitro. *J. Immunol. Methods* 204, 205–208.

(32) Gaber, R. F., Styles, C. A., and Fink, G. R. (1988) TRK1 encodes a plasma membrane protein required for high-affinity potassium transport in *Saccharomyces cerevisiae*. *Mol. Cell. Biol.* 8, 2848–2859.

(33) Loukin, S. H., Vaillant, B., Zhou, X. L., Spalding, E. P., Kung, C., and Saimi, Y. (1997) Random mutagenesis reveals a region important for gating of the yeast K<sup>+</sup> channel Ykc1. *EMBO J.* 16, 4817–4825.

(34) Zhang, J. H., Chung, T. D., and Oldenburg, K. R. (1999) A simple statistical parameter for use in evaluation and validation of high throughput screening assays. *J. Biomol. Screening* 4, 67–73.

(35) Xiong, Q., Gao, Z., Wang, W., and Li, M. (2008) Activation of Kv7 (KCNQ) voltage-gated potassium channels by synthetic compounds. *Trends Pharmacol. Sci.* 29, 99–107.

(36) Cohen, A., Ben-Abu, Y., Hen, S., and Zilberberg, N. (2008) A novel mechanism for human K2P2.1 channel gating. Facilitation of C-type gating by protonation of extracellular histidine residues. *J. Biol. Chem.* 283, 19448–19455.

(37) Goldstein, S. A., Bayliss, D. A., Kim, D., Lesage, F., Plant, L. D., and Rajan, S. (2005) International Union of Pharmacology. LV. Nomenclature and molecular relationships of two-P potassium channels. *Pharmacol Rev* 57, 527–540.

(38) Chemin, J., Patel, A. J., Duprat, F., Lauritzen, I., Lazdunski, M., and Honore, E. (2005) A phospholipid sensor controls mechanogating of the K<sup>+</sup> channel TREK-1. *EMBO J.* 24, 44–53.

(39) Honore, E., Maingret, F., Lazdunski, M., and Patel, A. J. (2002) An intracellular proton sensor commands lipid- and mechano-gating of the K(+) channel TREK-1. *EMBO J.* 21, 2968–2976.

(40) Segal-Hayoun, Y., Cohen, A., and Zilberberg, N. (2010) Molecular mechanisms underlying membrane-potential-mediated regulation of neuronal K2P2.1 channels. *Mol. Cell. Neurosci.* 43, 117–126.

(41) Rapedius, M., Schmidt, M. R., Sharma, C., Stansfeld, P. J., Sansom, M. S., Baukowitz, T., and Tucker, S. J. (2012) State-independent intracellular access of quaternary ammonium blockers to the pore of TREK-1. *Channels (Austin)* 6, 473–478.

(42) Lopes, C. M., Gallagher, P. G., Buck, M. E., Butler, M. H., and Goldstein, S. A. (2000) Proton block and voltage gating are potassium-dependent in the cardiac leak channel Kcnk3. *J. Biol. Chem.* 275, 16969–16978.

(43) Lopes, C. M., Zilberberg, N., and Goldstein, S. A. (2001) Block of Kcnk3 by protons. Evidence that 2-P-domain potassium channel subunits function as homodimers. *J. Biol. Chem.* 276, 24449–24452.

(44) Yuill, K. H., Stansfeld, P. J., Ashmole, I., Sutcliffe, M. J., and Stanfield, P. R. (2007) The selectivity, voltage-dependence and acid sensitivity of the tandem pore potassium channel TASK-1: contributions of the pore domains. *Pflugers Arch.* 455, 333–348.

(45) Niemeyer, M. I., Cid, L. P., Pena-Munzenmayer, G., and Sepulveda, F. V. (2010) Separate Gating Mechanisms Mediate the Regulation of K2P Potassium Channel TASK-2 by Intra- and Extracellular pH. *J. Biol. Chem.* 285, 16467–16475.

(46) Nayak, T. K., Harinath, S., Nama, S., Somasundaram, K., and Sikdar, S. K. (2009) Inhibition of human two-pore domain K<sup>+</sup> channel TREK1 by local anesthetic lidocaine: negative cooperativity and half-sites saturation kinetics. *Mol. Pharmacol.* 76, 903–917.

(47) Takahira, M., Sakurai, M., Sakurada, N., and Sugiyama, K. (2005) Fenamates and diltiazem modulate lipid-sensitive mechanogated 2P domain K(+) channels. *Pflugers Arch.* 451, 474–478.

(48) Cadaveira-Mosquera, A., Ribeiro, S. J., Reboreda, A., Perez, M., and Lamas, J. A. (2011) Activation of TREK currents by the neuroprotective agent riluzole in mouse sympathetic neurons. *J. Neurosci.* 31, 1375–1385.

(49) Lopes, C. M., Rohacs, T., Czirjak, G., Balla, T., Enyedi, P., and Logothetis, D. E. (2005) PIP2 hydrolysis underlies agonist-induced inhibition and regulates voltage gating of two-pore domain K<sup>+</sup> channels. *J. Physiol.* 564, 117–129.

(50) Sandoz, G., Douguet, D., Chatelain, F., Lazdunski, M., and Lesage, F. (2009) Extracellular acidification exerts opposite actions on TREK1 and TREK2 potassium channels via a single conserved histidine residue. *Proc. Natl. Acad. Sci. U.S.A.* 106, 14628–14633.

(51) Tertyshnikova, S., Knox, R. J., Plym, M. J., Thalody, G., Griffin, C., Neelands, T., Harden, D. G., Signor, L., Weaver, D., Myers, R. A., and Lodge, N. J. (2005) BL-1249 [(5,6,7,8-tetrahydro-naphthalen-1-yl)-[2-(1H-tetrazol-5-yl)-phenyl]-amine]: a putative potassium channel opener with bladder-relaxant properties. *J. Pharmacol. Exp. Ther.* 313, 250–259.